Chemical polishing method of GaAs specimens for transmission electron microscopy

Yue-Han Wu *, Li Chang

Department of Materials Science and Engineering, National Chiao Tung University, Hsinchu 300, Taiwan

ARTICLE INFO

ABSTRACT

A practical method for transmission electron microscopy specimen preparation of GaAs-based materials with quantum dot structures is presented to show that high-quality image observations in high-resolution transmission electron microscopy (HRTEM) can be effectively obtained. Specimens were prepared in plan-view and cross-section using ion milling, followed by two-steps chemical fine polishing with an ammonia solution (NH_4OH) and a dilute H_2SO_4 solution. Measurements of electron energy loss spectroscopy (EELS) and atomic force microscopy (AFM) proved that clean and flat specimens can be obtained without chemical residues. HRTEM images show that the amorphous regions of carbon and GaAs can be significantly reduced to enhance the contrast of lattice images of GaAs-based quantum structure.

Crown Copyright © 2009 Published by Elsevier Ltd. All rights reserved.

1. Introduction

High-resolution transmission electron microscopy (HRTEM) is an important and powerful technique for characterization of advanced materials and structures at atomic scale, which always requires the highest quality TEM specimens, particularly for compound semiconductors with quantum structures. In general, the TEM specimen has to be thin, contamination-free, and without artifacts from specimen preparation. For GaAs-based structures, the TEM specimen preparation has been conventionally performed using various methods, including chemical polishing, ion milling, and mechanical methods. Ion milling and focused ion beam (FIB) methods are popular in the recent decade for integrated circuit (IC) and light-emitting diode (LED) devices (Stevie et al., 1995). For FIB using a Ga^+ ion beam, GaAs is easily damaged with Ga^+ ion irradiation, and the Ga^+ ions may be incorporated into the GaAs which alters the original chemical composition, even though FIB can do precision specimen preparation (Rubanov and Munroe, 2005; Yabuuchi et al., 2004). These two drawbacks are unfavorable for HRTEM observations and chemical analysis. To reduce ion beam damage and to improve surface roughness of specimens, low energy ion milling with an energy less than 1000 eV has recently been developed (Barna et al., 1998 and Barna et al., 1999). However, the damage caused by lower energy ion milling is still more severe than chemical wet etching, and the composition of the specimen is also modified after ion bombardment (Dienelt et al., 2005; Sullivan et al., 1995). Alternatively, a mechanical method

which is called the 90° wedge method allows a clean specimen to be obtained from cleavage in {1 1 0} planes (Kakibayashi and Nagata, 1985; Williams and Carter, 1996). Although this method provides a TEM specimen almost without damage, it is limited by native cleavage orientations which only works for image observation along GaAs⟨1 1 0⟩, and may not be suitable for cases that observations have to be made along other directions such as ⟨1 0 0⟩. Chemical etching and polishing have been used for thinning TEM specimens after mechanical polishing in the early development of TEM (Irving, 1961). In the literature, one can find that various chemical solutions have been used in GaAs device etching and patterning processes for the past decades, including H_2SO_4, H_3PO_4, and NH_4OH with H_2O_2 and H_2O (Liu et al., 1999; Moon et al., 1998; Uenishi et al., 1994). Some of the solutions have also applied to TEM specimen preparation for GaAs-based materials (Ikarashi et al., 1992; Litvinov et al., 2008). However, it is not clear about the quality of the specimen and residues left on the surfaces after chemical treatments which are particularly vital for HRTEM. To improve the quality of HRTEM images, it is necessary to have smooth surfaces and remove covered amorphous layers. Here, we present a practical method which uses chemical fine polishing after conventional ion milling to obtain high-quality thin specimens of GaAs-based materials, and the results of HRTEM image observations and chemical analyses are shown for the effect of ion-induced amorphous GaAs layer.

2. Experimental procedures

TEM specimens in plan-view and cross-section were prepared from (0 0 1) GaAs wafers and InAs/GaAs quantum dot structures. The InAs/GaAs quantum dot structures were deposited by

* Corresponding author. Tel.: +886 3 5712121x 55373; fax: +886 3 5724727.
E-mail address: yhwu.mse91g@nctu.edu.tw (Y.-H. Wu).

molecular beam epitaxy (MBE) technique (Wu et al., 2008). HRTEM observations were performed in a JEOL 2010F microscope (C_s = 1.0 mm, 0.23 nm point resolution and 0.1 nm line resolution) equipped with a Gatan GIF imaging filter, and the images were recorded on a Gatan Ultrascan 2 k × 2 k CCD camera at 1000 k magnification (80 k on the microscope screen) with exposure time of 1 s. All the HRTEM images shown in this article are presented as raw data without any further imaging processing. Measurements of surface roughness were carried out using a Veeco Dimension 3100 scanning probe microscope in tapping mode of AFM with a tip of a diameter of 2 nm.

The details of TEM specimen preparation are described as following. A piece of sample in a size of 0.5×0.3 cm^2 with 0.35 mm thickness was cut from a GaAs wafer using a diamond scribing pen. For cross-sectional specimen preparation, additional four dummy pieces of Si in the same size were glued with the GaAs sample and used as polishing reference for thickness evaluation. Before gluing, they were thoroughly cleaned in acetone with an ultrasonic cleaner. An epoxy adhesive was prepared by mixing Epoxy Bond 110, Part A and Part B (Allied High Tech Products, Inc.) in a ratio of 10:1. After gluing of the five pieces together in sandwich, the sample was placed on a hot plate at 100 °C for 30 min. Then, the sample in plan-view or cross-section was mounted on a bipod polisher holder (Fig. 1) using a thermal wax for fixing with a piece of glass ground edge. Basically, the bipod holder has similar functions to the tripod one, and only two adjustable controllers have the better convenience to make a wedge-shaped specimen. Mechanical thinning to about 1–2 mm thickness was done from one side of the sample with SiC sand papers until 4000 grit, followed by thinning using diamond lapping discs (3 M Imperial^{TM} Diamond Lapping Film) of 30, 6, 3, 1 and 0.5 μm sized particles in sequence. The other side was then grinded and polished in the same process until the thickness was reduced to a few hundred nanometers. Here, it is noted that a small polishing angle with the horizontal adjustment of the two controllers can obtain a flat and thin specimen suitable for TEM observation in a widely large area. For successful preparation, the diamond lapping discs has to be constantly kept clean, i.e. the diamond particles and polished pieces scraped off the disc have to be removed; otherwise, they often result in severe scratches and even cracks on the GaAs which is brittle and mechanically vulnerable. For cross-section preparation, the dummy Si pieces were then used for monitoring the sample thickness (Mccaffrey and Hulse, 1998). When the color of the Si edges turned from dark red to light orange in the viewport of the bipod, the sample thickness might be approximately several hundred nanometers. After mechanical thinning, the sample was mounted on a Mo TEM grid instead of a Cu grid to reduce the contamina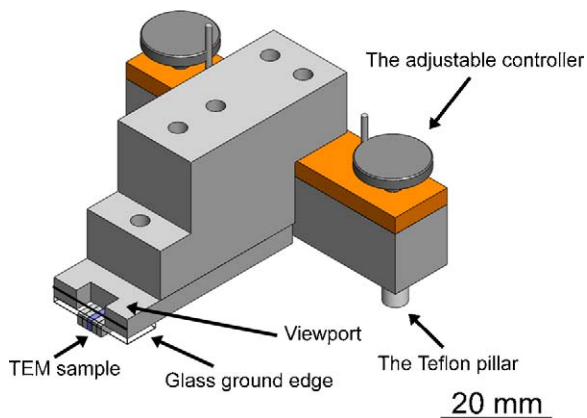tion from re-deposition during ion milling because of the lower sputtering yield of Mo than Cu. Another advantage is that Mo has strong chemical resistance to chemical etching.

For electron transparency of the specimen, ion beam milling was carried out in a Gatan PIPS system. In the present work, 3–5 keV Ar ion energy with incident angle of 3–5° and rotation speed of 3 rpm was used, which normally took 5–10 min to obtain perforation. For conventional bright-field and dark-field TEM image observations, the TEM specimen of 100–200 nm thickness is thin enough. However, it often requires a thickness less than 50 nm for HRTEM which imposes a more stringent condition for specimen preparation, particularly for quantum-structured specimens. The main issues for ion milling of a thin specimen are excessive beam damage which may cause the top and bottom surfaces to become amorphous, oxidized, and rough.(Singer et al., 1981; Barna et al., 1998) As the amorphous layers cover on the specimen, it often results in blurring of a HRTEM image and degradation of the resolution.

To effectively remove the surface layers, we developed a practical chemical polishing method for the final steps in TEM specimen preparation. The optimized experimental conditions are given in the following. We first dipped the ion-milled TEM specimen into aqueous ammonia solution (30% NH$_4$OH) for 1 min, followed by dipping into a dilute H$_2$SO$_4$ solution (1% H$_2$SO$_4$ in deionized water) for 10 min at room temperature. Finally, the specimen was cleaned with acetone and ethanol. After finishing chemical treatment, the specimen has to be carefully lifted from the surface of these solutions in a vertical angle to avoid the breakdown of the thin specimen resulted from the capillary effect.

3. Results and discussion

Fig. 2(a) and (e) show typical HRTEM images of GaAs (0 0 1) wafers in [0 0 1] and [1 1 0] zone axes, respectively, obtained from the correspondingly oriented specimens which were immediately inserted into the TEM just after ion milling at 4 keV ion energy and 4° incident angle for 10 min. In both HRTEM images, it can be seen that there are three distinct features. Around the edge, the light contrast of 5–6 nm width arises from amorphous carbon which might be formed from residues of chemicals and hydrocarbon molecules in the vacuum of the ion miller during ion bombardment. In the middle region of the images, a region of 10 nm width with darker contrast is seen with amorphous characteristics, that is mainly a GaAs amorphous layer as a result of radiation damage during ion milling. Amorphization of GaAs is well known in sputtering of GaAs with an Ar ion beam in the range of 1–10 keV (Malherbe, 1994). On the right hand side of the image in Fig. 2(a), even though lattice fringes exhibit blurred weak contrast, it still can recognized those regions where correspond to crystalline GaAs, as supported by the evidence of an enlarged HRTEM image in the inset. The result implies that the specimen is covered with amorphous layers of carbon and GaAs, which may impair HRTEM observations seriously. After chemical polishing, the specimens prepared are able to effectively expose lattice information in much better visibility with sharp contrast as shown in Fig. 2(c) and (g) taken from specimens in [0 0 1] and [1 1 0] orientations, respectively. It is clearly seen in both cases that the width of amorphous carbon is reduced to ∼3 nm and the amorphous GaAs is almost eliminated, thus allowing the significant improvement of imaging resolution. The fast-Fourier-transform (FFT) patterns of GaAs crystalline regions Fig. 2(a), (c), (e) and (g) are shown in Fig. 2(b), (d), (f) and (h), respectively. The strong effect of amorphous layers can be seen as diffuse noise in Fig. 2(b) and (f) which degrades the resolution. After chemical polishing, the diffraction spots with the weak amorphous effect are strong and sharp in Fig. 2(d) and (h). The FFT pattern in Fig. 2(d) clearly illustrates {4 0 0} spots with higher index spots which are absent
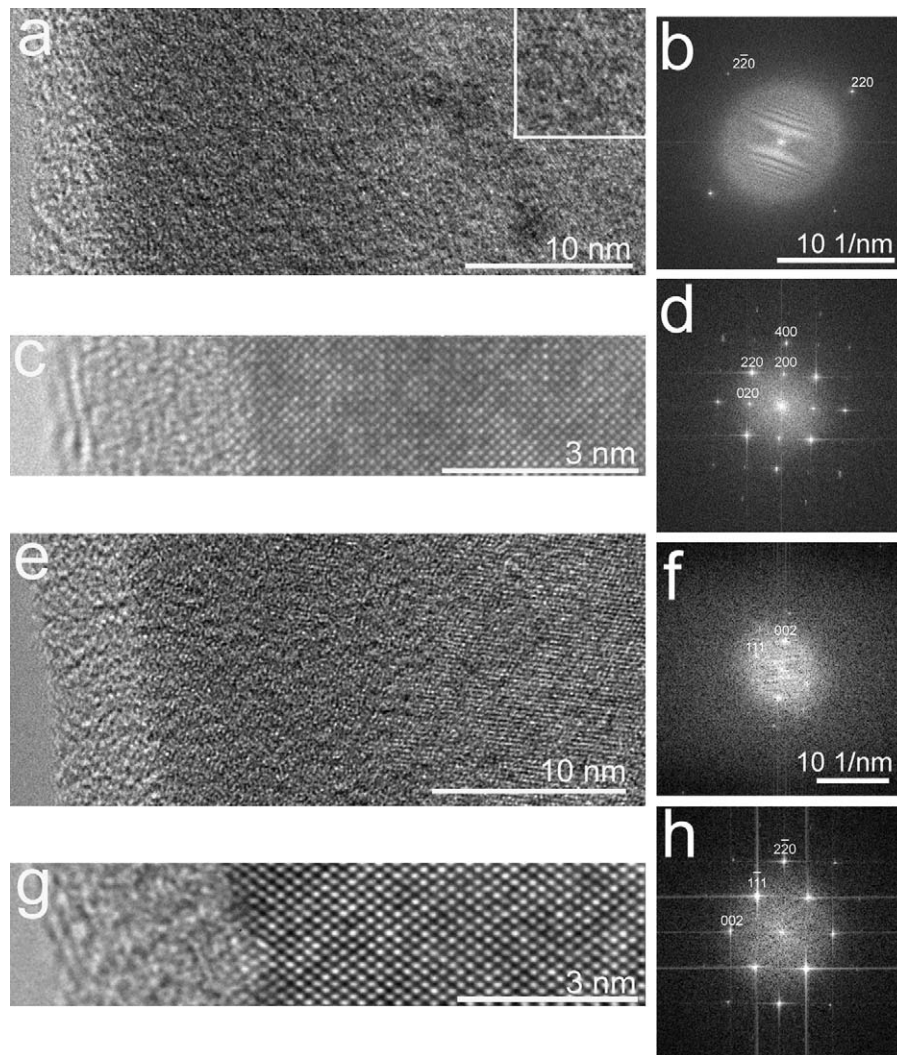

Fig. 1. Schematic drawing of a bipod for mechanical polishing.

The adjustable controller

Viewport

TEM sample   Glass ground edge   The Teflon pillar

20 mm

Fig. 2. (a) and (c) HRTEM images around the edge of a GaA specimen viewed in [0 0 1] zone axis after ion milling and after chemical polishing, respectively. Specimen prepared in [0 0 1] plan-view. The inset in (a) showing an enlarged lattice image from the right-hand side of (a). (e) and (g) HRTEM around the edge of a GaAs specimen viewed in the [1 1 0] zone axis after ion milling and after chemical polishing, respectively. Specimen prepared in [1 1 0] cross-section. (b), (d), (f), and (h) showing FFT patterns from crystalline areas in HRTEM images of (a), (c), (e), and (g), respectively.

in Fig. 2(d), suggesting that imaging resolution has been much improved. For the GaAs specimens prepared for observation in [1 1 0] zone axis, similar results are observed as shown in Fig. 2(h) in comparison with Fig. 2(f).

Electron energy loss spectroscopy (EELS) is a powerful technique for chemical analysis. Fig. 3(a) and (b) show EELS spectra from crystalline GaAs regions obtained in the same acquisition condition from specimens with and without chemical polishing The integrated signal intensity of carbon significantly decreases after chemical polishing, consistent with the observations of the decrease of the width of the carbon layer around the edge of the specimen (Fig. 2). Quantitative analysis of carbon composition in Fig. 3(a) shows the areal density of the specimen before chemical polishing is 3.11×10^5 atoms/nm^2, and after chemical polishing it is 2.85×10^5 atoms/nm^2. Also, both specimens exhibit similar carbon edge shape at the same energies. Hence, it is suggested that the characteristics of amorphous carbon have not significantly changed with chemical polishing. The above HRTEM and EELS results clearly demonstrate that the chemical treatment is effective to reduce amorphous carbon on the specimen surfaces. In Fig. 3(b), the top EELS spectrum from a crystalline region of GaAs after ion milling exhibits Ga, As, and oxygen K-edge signals, implying that GaAs specimens may have

been oxidized after milling. As Ar$^+$ ion milling has been proven to remove GaAs oxidized layers effectively (Pan et al., 1997), we believe that oxidation results from the exposure of the specimen to the ambient before loading into the microscope. It has been shown that the surface of a GaAs specimen after Ar$^+$ ion bombardment becomes As-deficient, and the Ga-rich surface is then easily oxidized (Sullivan et al., 1995; Chang et al., 1977). After dipping the ion-milled specimen into chemical solutions as the final step of the specimen preparation, oxygen K-edge signal disappears as shown in the button spectrum in Fig. 3(b). Therefore, the surface oxide has been effectively reduced to the concentration below the EELS detection limit, consistent with previous surface analysis studies (Chang et al., 1977; Lebedev et al., 2004) in which the aqueous ammonia solution was used for etching of GaAs to remove native oxide layers from GaAs (Chang et al., 1977; DeSalvo et al., 1996; Ensling et al., 2003; Bryce and Berk, 1996). Also, it has been found that the carbon coverage on GaAs surface can be reduced dramatically using H$_2$SO$_4$ solution (Liu et al., 2003a,b). It has been suggested that the GaAs surface may cover with an excess elemental arsenic layer of a thickness much less than 1 nm after wet etching using aqueous ammonia (ammonia hydroxide) and H$_2$SO$_4$ solutions (Lebedev et al., 2004; Ensling et al., 2003; Liu et al., 2003a,b). As a result, the elemental arsenic layer may prevent
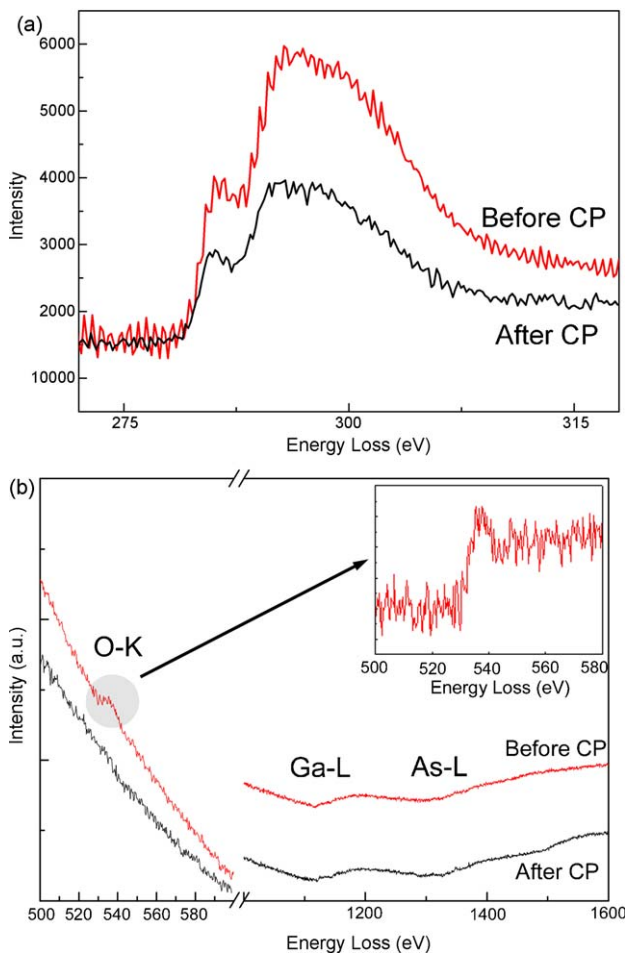
Fig. 3. (a) Carbon K-edge in EELS spectra obtained from specimens with and without chemical polishing of GaAs [1 1 0] specimen. (b) EELS spectra showing oxygen K-edge with Ga and As L edges before chemical polish (CP) and after CP.

formation of As oxidized layers (Liu et al., 2003a,b). Compared with the EELS spectrum without chemical polishing, L-edges of gallium and arsenic are clearly displayed with improved jump ratio in the spectrum from chemical-polished specimen, and no sulfur and nitrogen edges (not shown) have been found in the spectra examined, suggesting that the residual concentration of sulfur and nitrogen is below the detection limit of EELS as well.

Surface roughness of the TEM specimen is also important for HRTEM observations. Fig. 4(a)–(c) are AFM images of GaAs (0 0 1) the same sample treated in sequence, showing the surface morphologies in 1 μm² area after mechanical polishing, ion milling, and final chemical polishing, respectively. After mechanical polishing, the mirror-like surface is visible, and the root-mean-square (rms) roughness is about 4.2 nm as shown in Fig. 4(a). In

fact, mechanical polishing brings the eminent vertical difference (peak-to-valley) in the surface height of 18.5 nm in ~0.1 μm region. Then, the ion milling process results in the surface with long undulation of 0.2–03 μm period as shown in Fig. 4(b), while the vertical height difference becomes greater (roughness = 6.0 nm). Lastly, the smoothest surface can be obtained after chemical polishing as presented in Fig. 4(c), which shows the roughness of about 2.9 nm. In some local regions, smaller roughness of about 1.5 nm within 0.25 μm² can even be seen.

The same procedure has been applied on TEM specimen preparation of InAs/GaAs quantum dot structure for ⟨0 1 0⟩ HRTEM observations. In general, the quantum dots and the wetting layers consist of InGaAs compositions with larger lattice than GaAs. Comparison of HRTEM images obtained from the same specimen without and after chemical polish is made near the same area. Fig. 5(a) shows a typical HRTEM image obtained from a thin region including an embedded InGaAs quantum dot with the underlying wetting layer after ion milling. Positions of InAs/GaAs quantum dots are easily found from the contrast in HRTEM images. The contrast of quantum dots mainly includes two different mechanisms, which are strain contrast and phase contrast. (De Giorgi et al., 2001; Scheerschmidt and Werner, 2002) Strain contrast showing the dark area arises from the large strain field around quantum dots, and phase contrast in HRTEM images due to atomic structure of the thin specimen is interference of lattice features. The contrast around the quantum dot and the wetting layer appears blurred in Fig. 5(a), resulting from the effects of amorphous carbon and GaAs surface layers. However, sharp image contrast can be clearly observed in HRTEM images obtained from the same specimen after chemical polishing, as shown in Fig. 5(b) and (c) which are recorded raw data (without any digital image processing with filters) of the same quantum dot embedded in the GaAs matrix and the wetting layer, respectively. The sharp lattice image contrast in the Fig. 5(b) unambiguously reveals the In-rich dot has a larger lattice spacing than the GaAs matrix, and the lattice image pattern of the dot exhibits a different arrangement from that of the matrix. Also, the strain contrast due to the dot is also demonstrated. In Fig. 5(b), the dark areas as pointed by the white arrows illustrate the region mainly due to strain contrast, because formation of embedded InAs QDs of larger lattices in GaAs leads to the local strain field with QDs. (De Giorgi et al., 2001; Scheerschmidt and Werner, 2002) Compared with Fig. 5(a), it is noted that the strain contrast can be altered after ion milling. From the above observations, the shape of the dot can thus be determined to be like truncated-pyramid and the size in 4 nm height and 12 nm width. Also, the observation of the wetting layer is also clearly seen (as indicated between white arrows) in Fig. 5(c) from which we can determine its thickness in three monolayers. Furthermore, after image processing and analysis using the Wiener filter one can estimate the improvement of the image signal-to-noise ratio from the same area when comparison is made on Fig. 5(a) and (b) in about 1.4 times. From the image observation of the contrast of dot and wetting layer, it is speculated that the chemical polishing
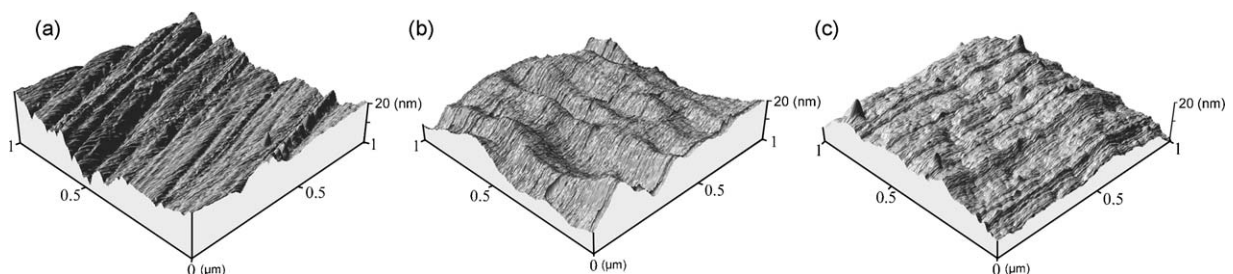

Fig. 4. AFM images of GaAs (0 0 1) in 1 μm² illustrating the surface morphology (a) after mechanical polishing, (b) after ion milling, and (c) after chemical polishing.
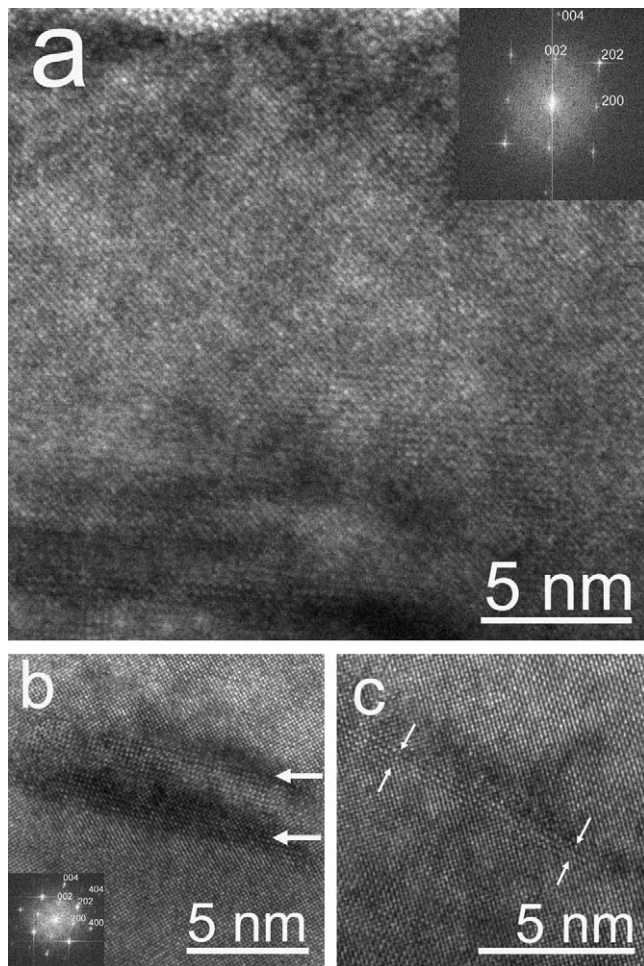
Fig. 5. (a) HRTEM image of a quantum dot near the edge of the InAs/GaAs specimen in [0 1 0] zone axis. (b) HRTEM image showing the same dot in (a), and (c) HRTEM image of the wetting layer after chemical polishing of the same specimen in (a). The dark area as pointed with white arrows in (b) showing strain contrast about the quantum dots. The wetting layer in (c) is illustrated at the location between the white arrows.

properties of the InGaAs in NH_4OH and H_2SO_4 is not significantly different from those of GaAs.

Chemical etching of GaAs with NH_4OH and H_2SO_4 with hydrogen peroxide (H_2O_2) has been commonly used for IC and LED device processing (Ishikawa et al., 1989; Johnson et al., 1991). However, the recipe of chemical polishing used in this study focuses on the characteristics of the process for TEM specimen preparation. Usually, use of H_2O_2 can activate chemical-etching reactions, but it has been proven to form surface oxide layers, especially at concentration greater than 2% (Hue et al., 1998). Also, solution of H_2SO_4 and H_2O_2 has a similar etching effect with faster etching rate, which means the control of the etching time and chemical concentration has to be precise to avoid the removal of the thin areas for electron transparency (Barycka and Zubel, 1987). In addition, the etching selectivity for GaAs-based heterostructure materials increases with H_2O_2 concentration, which leads to a rougher specimen surface (Kitano et al., 1997). To obtain a smooth and clean surface on a TEM specimen for HRTEM observation, we used the dilute solution of NH_4OH and H_2SO_4 with H_2O only for fine control of the polishing. Moreover, it has also been found that the applied sequence of NH_4OH and H_2SO_4 solutions is important for the quality of TEM specimens. In our experience, if we used dilute H_2SO_4 solution directly after ion milling, the amorphous carbon could be significantly decreased around the edge regions; never-

theless, the amorphous GaAs still remained near the edge. The following usage of 30% NH_4OH could not provide fine polishing to smooth the surface further, even though the amorphous GaAs was removed. As a result, the surface roughness was similar to that after ion milling, so that there was only a much smaller area being useful for HRTEM observation without contrast variations.

4. Summary

Chemical polishing with NH_4OH and H_2SO_4 in two-steps after conventional ion milling is an effective and practical TEM specimen preparation method for GaAs-based materials to obtain improved image quality. We have demonstrated that this method can remove significant amounts of amorphous phases of carbon and GaAs resulted from the conventional process, and a smoother surface of the TEM specimen can be obtained, such that high-quality HRTEM image observations can be made on embedded InAs/GaAs quantum dot structure.

References

Barna, A., Pece, B., Menyhard, M., 1998. Amorphisation and surface morphology development at low-energy ion milling. Ultramicroscopy 70, 161–171.

Barna, A., Pece, B., Menyhard, M., 1999. TEM sample preparation by ion milling/ amorphization. Micron 30, 267–276.

Barycka, I., Zubel, I., 1987. Chemical etching of (1 0 0) GaAs in a sulphuric acid-hydrogen peroxide-water system. J. Mater. Sci. 22, 1299–1304.

Bryce, C., Berk, D., 1996. Kinetics of GaAs sdissolution in H_2O_2-NH_4OH-H_2O solutions. Ind. Eng. Chem. Res. 35, 4464–4470.

Chang, C.C., Citrin, P.H., Schwartz, B., 1977. Chemical preparation of GaAs surfaces and their characterization by Auger electron and X-ray photoemission spectroscopies. J. Vac. Sci. Technol. 14, 943–952.

De Giorgi, M., Taurino, A., Passaseo, A., Catalano, M., Cingolani, R., 2001. Interpretation of phase and strain contrast of TEM images of InxGa1ÀxAsÕGaAs quantum dots. Phys. Rev. B. 63, 2453021–2453029.

DeSalvo, G.C., Bozada, C.A., Ebel, J.L., Look, D.C., Barrette, J.P., Cerny, C.L.A., Dettmer, R.W., Gillespie, J.K., Havasy, C.K., Jenkins, T.J., Nakano, K., Pettiford, C.I., Quach, T.K., Sewell, J.S., Via, G.D., 1996. Wet chemical digital etching of GaAs at room temperature. J. Electrochem. Soc. 143, 3652–3656.

Dienelt, J., Zimmer, K., Sonntag, J. von, Rauschenbach, B., Bundesmann, C., 2005. Roughness and damage of a GaAs surface after chemically assisted ion beam etching with Cl_2/Ar^+. Microelectron. Eng. 78-79, 457–463.

Ensling, D., Hunger, R., Kraft, D., Mayer, T., Jaegermann, W., Rodrigues-Girones, M., Ichizli, V., Hartnagel, H.L., 2003. Pulse plating of Pt on n-GaAs (1 0 0) wafer surfaces: synchrotron induced photoelectron spectroscopy and XPS of wet fabrication processes. Nucl. Istrum. Methods Phys. Res. Sect. B-Beam Interact. Mater. Atoms 200, 432–438.

Hue, X., Boudart, B., Crosnier, Y., 1998. Gate recessing optimization of GaAs/Al_0 $_{22}Ga_0$ $_{78}$As heterojunction field effect transistor using citric acid/hydrogen peroxide/ammonium hydroxide for power applications. J. Vac. Sci. Technol. B 16, 2675–2679.

Ikarashi, N., Tanaka, M., Sakaki, H., Ishida, K., 1992. High-resolution electron microscopy of growth interruption effect on AIAs/GaAs interfacial structure during molecular beam epitaxy. Appl. Phys. Lett. 60, 1360–1362.

Irving, B.A., 1961. The preparation of thin films of germanium and silicon. Br. J. Appl. Phys. 12, 92–93.

Ishikawa, J., Ito, T., Oh-iso, Y., Yamamoto, M., Shin-ichi Takahashi, N., Kurita, S., 1989. Lasing characteristics of 0.8 μm InGaAsP/GaAs lasers fabricated by wet chemical etching. J. Appl. Phys. 65, 3767–3772.

Johnson, M.J., Kuhn, K.J., Darling, R.B., 1991. Effect of etch treatment prior to Schottky contact fabrication on In_0 $_{05}Ga_0$ $_{95}$As. Appl. Phys. Lett. 58, 1893–1895.

Kakibayashi, H., Nagata, K., 1985. Composition dependence of equal thickness fringes in an electron microscope image of GaAs/Al_xGa_{1-x} As multilayer structure. Jpn. J. Appl. Phys. 24, L905–L907.

Kitano, T., Izumi, S., Minami, H., Ishikawa, T., Sato, K., Sonoda, T., Otsubo, M., 1997. Selective wet etching for highly uniform GaAs/Al_0 $_{15}Ga_0$ $_{85}$As heterostructure field effect transistors. Vac. Sci. Technol. B 15, 167–170.

Lebedev, M.V., Ensling, D., Hunger, R., Mayer, T., Jaegermann, W., 2004. Synchrotron photoemission spectroscopy study of ammonium hydroxide etching to prepare well-ordered GaAs (1 0 0) surfaces. Appl. Surf. Sci. 229, 226–232.

Litvinov, D., Blank, H., Schneider, R., Gerthsen, D., Vallaitis, T., Leuthold, J., Passow, T., Grau, A., Kalt, H., Klingshirn, C., Hetterich, M., 2008. Influence of InGaAs cap layers with different In concentration on the properties of InGaAs quantum dots. J. Appl. Phys. 103, 0835321–0835323.

Liu, H.C., Tsai, S.H., Hsu, J.W., Shih, H.C., 1999. The phase identification of the H_2SO_4-etched GaAs by X-ray diffraction. Mater. Chem. Phys. 61, 117–123.

Liu, Z., Sun, Y., Machuca, F., Pianetta, P., Spicer, W.E., Pease, R.F.W., 2003a. Optimization and characterization of III–V surface cleaning. J. Vac. Sci. Technol. B 21, 1953–1958.

Liu, Z., Sun, Y., Machuca, F., Pianetta, P., Spicer, W.E., Pease, R.F.W., 2003b. Preparation of clean GaAs (1 0 0) studied by synchrotron radiation photoemission. J. Vac. Sci. Technol. A 21, 212–218.

Malherbe, J.B., 1994. Sputtering of compound semiconductor surfaces I. Ion-solid interactions and sputtering yields. Crit. Rev. Solid State Mater. Sci. 19, 55–127.

Mccaffrey, J.P., Hulse, J., 1998. Transmitted color and interference fringes for TEM sample preparation of silicon. Micron 29, 130–144.

Moon, E.A., Lee, J.L., Yoo, H.M., 1998. Selective wet etching of GaAs on $Al_xGa_{1-x}As$ for AlGaAs/InGaAs/AlGaAs pseudomorphic high electron mobility transistor. J. Appl. Phys. 84, 3933–3938.

Pan, J.S., Weey, A.T.S., Huan, C.H.A., Tan, H.S., Tan, K.L., 1997. ARXPS analysis of surface compositional change in Ar^+ ion bombarded GaAs (1 0 0). J. Phys. D: Appl. Phys. 30, 2514–2519.

Rubanov, S., Munroe, P.R., 2005. Damage in III–V compounds during focused ion beam milling. Microsc. Microanal. 11, 446–455.

Scheerschmidt, K., Werner, P., 2002. Characterization of structure and composition of quantum dots by transmission electron microscopy. In: Nano-Optoelectronics: Concepts, Physics and Devices, Springer-Verlag, Heidelberg, pp. 67–98.

Singer, I.L., Murday, J.S., Cooper, L.R., 1981. Surface composition changes in GaAs due to low-energy ion bombardment. Surf. Sci. 108, 7–24.

Stevie, F.A., Shane, T.C., Kahora, P.M., Hull, R., Bahnck, D., Kannan, V.C., David, E., 1995. Applications of focused ion beams in microelectronics production. Surf. Interface Anal. 23, 61–68.

Sullivan, J.L., Yu, W., Saied, S.O., 1995. A study of the compositional changes in chemically etched, Ar ion bombarded and reactive ion etched GaAs (1 0 0) surfaces by means of ARXPS and LEIS. Appl. Surf. Sci. 90, 309–319.

Uenishi, Y., Tanaka, H., Ukita, H., 1994. Microstructure characterization of AlGaAs fabricated by AlGaAs/GaAs micromachining. IEEE Trans. Electron Devices 41, 1778–1783.

Williams, D.B., Carter, C.B., 1996. Transmission electron microscopy. Plenum, New York.

Wu, Y.H., Chang, L., Chen, L.C., Chen, H.S., Chen, F.R., 2008. Geometrical correlations of quantum dots in InAs/GaAs superlattice structure from electron tomography. Appl. Phys. Lett. 93, 1531081–1531083.

Yabuuchi, Y., Tametou, S., Okano, T., Inazato, S., Sadayama, S., Yamamoto, Y., Iwasaki, K., Sugiyama, Y., 2004. A study of the damage on FIB-prepared TEM samples of AlxGa1-xAs. J. Electron Microsc. 53, 471–477.